Biomed Microdevices (2006) 8:247–253
DOI 10.1007/s10544-006-8305-2

# Investigation of interaction between two neutralizing monoclonal antibodies and SARS virus using biosensor based on imaging ellipsometry

**Cai Qi · Jin-Zhu Duan · Zhan-Hui Wang · Yan-Yan Chen · Pan-He Zhang · Lin Zhan · Xi-Yun Yan · Wu-Chun Cao · Gang Jin**

Published online: 22 May 2006


**Abstract** Two neutralizing human scFv, b1 and h12 were identified initially using ELISA, employing highly purified virus as the coating antigen. The biosensor technique based on imaging ellipsometry was employed directly to detect two neutralizing monoclonal antibodies and serial serum samples from 10 SARS patients and 12 volunteers who had not SARS. Further, the kinetic process of interaction between the antibodies and SARS-CoV was studied using the real-time function of the biosensor. The biosensor is consistent with ELISA that the antibody h12 showed a higher affinity in encountering the virus than antibody b1. The affinity of antibody b1 and antibody h12 was $9.5 \times 10^6$ $M^{-1}$ and $1.36 \times 10^7$ $M^{-1}$, respectively. As a label free method, the biosensor based on imaging ellipsometry proved to be a more competent mechanism for measuring serum samples from SARS patients and the affinity between these antibodies and the SARS coronavirus.

**Keywords** SARS-CoV · ELISA · Biosensor · Neutralizing antibody · Dynamic process · Imaging ellipsometry

C. Qi · Z.-H. Wang · Y.-Y. Chen · G. Jin (✉)
Institute of Mechanics, Chinese Academy of Sciences, #15, Bei-si-huan West Rd., Beijing, 100080, China
e-mail: gajin@imech.ac.cn

J.-Z. Duan · X.-Y. Yan · G. Jin
Institute of Biophysics, Chinese Academy of Sciences, #15, Da-tun Rd., Beijing, 100101, China

C. Qi · Y.-Y. Chen
Graduate School of the Chinese Academy of Sciences, 19, Yu-quan Rd, Shi-jing-shan District, Beijing, 100049, P.R. China

P.-H. Zhang · L. Zhan · W.-C. Cao
Institute of Microbiology and Epidemiology, The Academy of Military Medical Sciences, #27 Taiping Rd., Beijing, 10085, China

## 1. Introduction

From November 2002 to July 2003, severe acute respiratory syndrome (SARS), caused by a novel coronavirus, quickly affected many countries and had a highly disruptive impact on people's lives as well as the economy. The most recent SARS outbreaks were reported in Beijing and Anhui Province, China, in April 2004. These indicated that SARS epidemics might recur at any time in the future (Peiris et al., 2003; Lingappa et al., 2004; Poutanen et al., 2003). Currently, a number of SARS vaccine candidates were being developed, which included inactivated SARS coronavirus (SARS-CoV) vaccines, DNA vaccines, and attenuated virus vaccines that produced SARS-CoV specific protein (Bisht et al., 2004; Bukreyev et al., 2004; Yang et al., 2004). However, their utility in humans remained unclear. Moreover, there had been grave concerns regarding their safety as some antigens to the virus. Some vaccines might elicit antibodies that did not neutralize (Oba et al., 2003; Wang et al., 2003a). Neutralizing the SARS-CoV infection through passive immunization of the antibodies carried a low level of risk compared with methods involving inactivated viruses or attenuated virus vectors (Wang et al., 2004a; Ter Meulen et al., 2004). Thus, the screening of new and effective antibodies and a deeper understanding of the antibodies' responses to the viral components of the virus were imperative for more accurate diagnosis of the illness and the development of a vaccine.

After the new neutralizing antibodies were screened, there were various immune methods available to detect their presence and measure their activity levels. The key methods were: enzyme-linked immunosorbent assay (ELISA), western blot (WB) (Wang et al., 2003a), indirect fluorescent antibody (IFA) (Wu et al., 2004), reverse transcription-polymerase chain reaction (RT-PCR) and real-time PCR (Poon et al.,

2004; Lau et al., 2003). These methods exhibited varied strengths and weaknesses. Most of these methods required the samples to be labeled, which occasionally resulted in a high percent of false positives or false negatives, and required expensive equipment (Long et al., 2004). Moreover, some procedures were a discontinuous method and kinetic information was not readily available by the possibility of mass transport limitations (Yu et al., 2004). In contrast with these methods, the biosensor with imaging ellipsometry offered several advantages such as it did not require the use of labels; it was rapid, intuitionistic and low cost. Furthermore, it could analyze directly the interactive process. The biosensor technique was developed in 1995 (Jin et al., 1995a). It was a protein analysis technique that was able to engage in swift, automated, multi-protein analysis simultaneously and which combined high spatial resolution imaging ellipsometry with microarray (Jin et al., 1996, 1995b). Previously, the technique had been used successfully in a number of scenarios, for example in, 1) human IgG molecules covalent immobilization (Wang and Jin, 2004b); 2) hormone detection (Zhao et al., 1998); 3) cell factor and its receptor interaction (Wang and Jin, 2002); 4) cancer marker test (Zhang et al., 2005); 5) quantitative protein competitive adsorption (Hofmann et al., 2002; Ying et al., 2002, 2004); 6) kinetic detection for multi-protein interaction process (Jin et al., 2003); 7) biomolecule interaction (Wang and Jin, 2003b).

For this study, an immune antibody phage-display library was constructed from B cells of SARS convalescent patients and more than eighty clones were selected from the library by using the whole inactivated SARS-CoV virions as target. Two human single chain Fv (scFv) b1 and h12 were characterized extensively (Duan et al., 2005, 2006). The biosensor was utilized to detect the activity of the new antibodies against the SARS-CoV in encountering the virus in contrast to the 10 serum samples from SARS-infected donors. Furthermore, real-time detection method the interaction between SARS-CoV and these new antibodies was also investigated.

## 2. Materials and methods

### 2.1. Materials and reagents

Silicon wafers were purchased from General Research Institute for Nonferrous Metals. Tween 20 was purchased from Sigma-Aldrich. 3-aminopropyltriethoxy-silane (99%, v/v) was purchased from ACROS. Glutaraldehyde (50% aqueous solution photographic GRA) and Bovine serum albumin (BSA) were purchased from SIGMA. All chemicals used were of analytical grade. Antibody b1 (137 $\mu$g/ml, MW 29KD) and antibody h12 (87.2 $\mu$g/ml, MW 29KD) and SARS-CoV were provided from the Institute of Biophysics, Chinese Academy of Sciences (Duan et al., 2005, 2006; Lin et al., 2004). Serum samples from 10 SARS patients were isolated from 7 to 210 days after the onset of the symptoms were provided from Department of Epidemiology, Institute of Microbiology and Epidemiology, Beijing, China. Clinical information of some patients was listed in the Table 1. Phosphate-buffered saline (PBS; 10 mM phosphate, 0.1 M NaCl pH7.2) and PBS with 1% tween 20 (PBST)were prepared. Deionized water (Resistivity18.3 MΩcm) was produced by ion exchange demineralization, followed by passing through a Milli-Q plus system from Millipore (Millipore, Bedford, MA). Real-time spectroscopic ellipsometry experiments were performed with a variable angle spectroscopic ellipsometer of J. A. Woollam Co.

**Table 1** The clinical information of SARS patients

| Number | Age | Sex | Time of presenting symptoms | Time of sampling |
|---|---|---|---|---|
| P002 | 50 | Woman | April 7, 2003 | April 19, 2003 |
| P004 | 69 | Woman | April 10, 2003 | April 19, 2003 |
| P005 | 41 | Man | April 8, 2003 | April 19, 2003 |
| P010 | 26 | Woman | April 4, 2003 | April 19, 2003 |
| YA014 | 80 | Man | April 4, 2003 | April 19, 2003 |
| YA004 | — | Man | April 1, 2003 | April 18, 2003 |
| YA023 | — | Man | March 21, 2003 | April 18, 2003 |

### 2.2. ELISA

96-well microtiter plates (Nunc, Rochester, NY) were coated overnight at 4° with inactivated SARS-CoV particles in 0.05 M $Na_2CO_3$, pH 9.6, blocked with 3% BSA in PBS, and incubated with an individual phage scFv in PBS containing 1% BSA. After washed with PBST, the bound antibodies were detected by HRP-conjugated anti-M13 antibody followed by incubation with ortho-phenylene-diamine (OPD) as substrate. The color reaction was measured at 490 nm in a BioRad ELISA reader (Hercules, CA, USA).

### 2.3. Biosensor technique

With the modified substrate of the silicon wafer with 3-aminopropyltriethoxy-silane and Glutaraldehyde, antibody (or antigen) can be covalently bound to different areas on surface of silicon wafer due to the reaction of the Schiff base with –CHO with a model of micro-fluidic for a microarray. In this case, each area of the microarray may function as an immune-probe. An immune-probe can capture corresponding antigens (or antibodies) in the solution. When the corresponding antibodies (or antigens) in the solution interact with the immune-probe in the microarray, they form a complex upon their affinity and the layer covering the surface area

of the interaction becomes thicker (or surface concentration higher). A significant increase in the attached layer thickness (or surface concentration) indicates that the solution contains the antibody (or antigen). The imaging ellipsometry is used to detect the protein layer pattern on the microarray surface. The distribution of the lateral thickness (or surface concentration) protein layer pattern is simultaneously detected, which may further point to the existence of antibodies in the tested solution for immune tests. During the binding process, the kinetic process of protein interactions also became observable with real-time spectroscopic ellipsometry. Some important kinetic data can be supplied using real-time experiments.

Imaging ellipsometry is an enhancement of standard single-beam ellipsometry which combines the power of ellipsometry with microscopy (Jin et al., 1996). Its technical details could be found in these literatures (Wang and Jin, 2003c; Arwin et al., 1993; Stenberg and Nygren, 1983).

### 2.4. Polished silicon wafer surface modification

Polished silicon wafer was chosen as substrate here. The silicon wafers were cut into rectangles 20 × 10 mm and cleaned in deionized water. The wafer surface was washed in solution (30% $H_2O_2$:98% $H_2SO_4$ = 1:3 v/v) for 30 min. The solution not only removed contaminants of the silicon surface, but also improved the number of silanol groups on the surface, thus making the surface hydrophilic. After being rinsed in deionized water and ethanol, the washed surfaces were incubated in a mixture of 3-Aminopropyltriethoxy-silane (APTES 99%, v/v) and absolute ethanol (3-Aminopropyltriethoxy-silane: absolute ethanol = 1:10 v/v) for 2 h. Following this, they were again rinsed in absolute ethanol three times. The reaction of 3-Aminopropyltriethoxy-silane with silanol groups on the surface of the wafer, resulted in the covalent immobilization of –O-Si$(OH)_2$-$(CH_2)_3NH_2$, which formed a layer of densely packed amino groups on a silicon dioxide layer, making the surface highly hydrophobic. After rinsed in ethanol and PBS, the washed surface was incubated in a mixture of Glutaraldehyde (50% aqueous solution photographic GRA) and PBS (Glutaraldehyde:PBS = 1:15 v/v) for 1 h. After rinsed in PBS, the silicon wafers were kept in PBS. $OHC(CH_2)_3CHO$ could react with $–NH_2$ of –O-Si$(OH)_2$-$(CH_2)_3NH_2$ and made $–(CH_2)_3N{=}CH(CH_2)_3CHO$ (Wang and Jin, 2004c).

### 2.5. Qualitative detection of serum and the antibody against SARS-CoV with biosensor based on imaging ellipsometry

SARS-CoV ligand immobilized was prepared and covalently immobilized on six individual areas on the surface of a modified silicon wafer with a model of micro-fluidic for a microarray. Each area required 10 $\mu$l of SARS-CoV, which passed the surface of modified silicon wafer at 1 $\mu$l/min, after which the wafers were rinsed with deionized water. After being blocked for 30 min at room temperature with 10 mg/ml BSA, six identical immune-probes were formed. Antibody h12 and b1 were diluted once using PBS solution with 1% tween 20 to the concentration 68.5 $\mu$g/ml and 43.6 $\mu$g/ml respectively. Each area required 10 $\mu$l of antibody, which passed through the surface of these immune-probes at 1 $\mu$l/min. Of the six areas, two were control areas, two areas were chosen to detect antibody h12 and two areas were chosen to detect antibody b1. Antibody h12 and b1 were detected twice to verify the immunoreactions within a microarray. After being rinsed with deionized water and dried with nitrogen, the surface concentration of surface-bound antibody against SARS-CoV was qualitatively detected using imaging ellipsometry. If the antibody in the solution and immune-probe formed a complex, the layer on the area would become thicker. Follow same step, the 10 serum samples from SARS infected donors and negative samples were detected using the biosensor. The detecting time was estimated to be around 10 min, with the whole process requiring approximately 40 min.

### 2.6. The kinetic process of analyzing the two antibodies against SARS-CoV using real-time spectroscopic ellipsometry

For the real-time observation of the interaction between the antibodies and the SARS virus, SARS-CoV ligand immobilized was prepared. This was achieved using the following process. Modified silicon wafer was incubated for 10 min with SARS-CoV, and SARS-CoV was covalently immobilized. Following this, the wafers were rinsed with deionized water and the surface containing immobilized SARS-CoV was then blocked using 10 mg/ml BSA for 30 min. The chip was inserted into a reaction cell containing buffer solution used in real-time experiments and the sensing surface was clearly observed. The antibody b1 and h12 were diluted to 82.2 $\mu$g/ml and 34 $\mu$g/ml in PBST, respectively. The solution containing the antibody was poured into the cell that already contained a buffer solution without antibodies. Some antibody molecules diffused to the sensing surface reacted with the corresponding antigens on the surface, resulting in the formation of their complexes. The concentration distribution of antibody in the cell reached to uniform. The binding process between antigen on the surface and antibodies in the solution was then observed simultaneously. The distribution of lateral thickness (or surface concentration) of protein layer pattern was detected and recorded once every 1.3 s, which corresponded to the speed of the reaction between the antibody and SARS-CoV. The binding process caused the surface concentration on the corresponding sensing surface to increase with time.

Similar to the BIAcore technique (Malmborg et al., 1992), the real time experiment was performed according to the

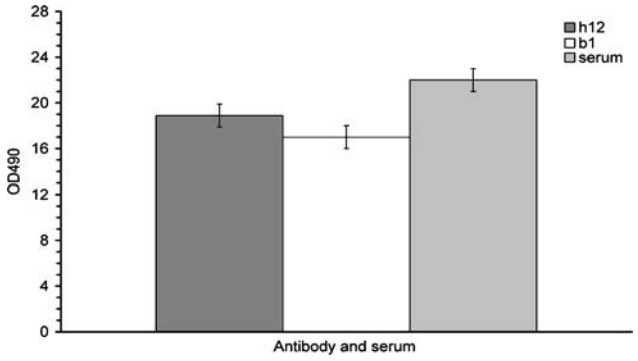


**Fig. 1** Detection activity of antibodies with ELISA contrast with serum. Antibody h12 OD is 1.85. Antibody b1 OD is 1.70. Serum SARS patient OD is 2.19

method described in the literature (Wang and Jin, 2003b). Rate constants for the interaction (association rate constant $k_a$ and dissociation rate constant $k_d$) were derived from an analysis of the binding curves in real-time experiment with spectroscopic ellipsometry. To interpret the sensorgram, first order kinetics was assumed and the association constant was given by:

$$dR/dt = k_a C R_{max} - (k_a C - k_d) R$$

where C was the concentration of analytes;

$R_{max}$ was the maximum analytes binding capacity on the biosensor surface;

R was the quantity of the analytes in chip at time t.

The association rate constant was calculated by plotting dR/dt against R, measuring the negative slope value ($= k_a C - k_d$) and plotting it against different concentrations of antibody/antigen. The slope gave the association rate constant. When using this evaluation method, it was not necessary for the interaction to reach equilibrium. The dissociation rate constant was calculated from the equation:

$$\ln(R_{A1}/R_{An}) = k_d \times (t_n - t_1)$$

where

$R_{A1}$ = bound analyte at time t = 1, the start of the dissociation;

$R_{An}$ = bound analyte at time t = n

The affinity constant was calculated from the association/dissociation rate constant.

## 3. Results

### 3.1. Screening of antibody against SARS-CoV with ELISA

The result of detection antibody b1, antibody h12 and SARS serum using ELISA is shown in Fig. 1. The optical density (OD) of serum SARS is the greatest. The OD of antibody h12 is greater than that of antibody b1.

### 3.2. Detection of serum of SARS patients and antibodies against SARS-CoV using the biosensor

The results are shown in Table 2. The Fig. 2 images in grayscale show in (A), (C) and the corresponding thickness distribution in three dimensions shows in (B), (D). Some significant increases in the layer thickness appear in the bioactive areas, as expressed in Fig. 3. After being blocked with 10 mg/ml BSA, the surface concentration of the SARS-CoV layer is 0.68 $\mu$g/cm$^2$. The surface concentration of antibody b1, antibody h12 and serum of SARS patient are 1.14, 0.9 and 0.96 $\mu$g/cm$^2$, respectively.

The results of serial serum samples from 10 SARS patients and 12 negative serum samples from volunteers who have not had SARS are shown in Table 3 and Fig. 4. The result shows that the film thickness of positive samples is obvious higher than the SARS-CoV and negative samples layer, and the thickness of negative samples layer for no positive interaction is similar to the SARS-CoV layer. Analytical sensitivity and detection limit of the biosensor can be found in the literature (Zhang et al., 2005).

### 3.3. The kinetic process analysis of antibody against SARS-CoV using real-time spectroscopic ellipsometry

Figures 5 and 6 show a series of increases in the surface concentration, allowing for the binding processes between antibody b1, antibody h12 and SARS-CoV. The experiment is repeated several times. The surface concentration increase indicates the point where the antibody binds to the ligand on their affinity. There are two interaction rates for the binding processes seen obviously below and over 300 s.

**Table 2** The thickness of antibodies and serum film on biosensor based on imaging ellipsometry

| SARS-CoV, antibody, serum | times | | | | | | | | | | | Average thickness (nm) |
|---|---|---|---|---|---|---|---|---|---|---|---|---|
| | 1 | 2 | 3 | 4 | 5 | 6 | 7 | 8 | 9 | 10 | 11 | |
| SARS-Cov | 5.3 | 5.1 | 6 | 5.7 | 5.2 | 5.1 | 6.5 | 5.2 | 6.6 | 5.5 | 6.2 | 5.7 |
| Antibody b1 | 9.9 | 9.6 | 8.7 | 9.2 | 10.4 | 8.7 | | | | 10.3 | 9.0 | 9.5 |
| Antibody h12 | 7.9 | | | 7.3 | 7.3 | 7.6 | 7.2 | | | | 7.8 | 7.5 |
| Serum SARS | 7.7 | 7.3 | 7.8 | 8.0 | | 8.0 | 7.8 | 7.8 | 8.9 | 9.0 | 7.8 | 8.0 |

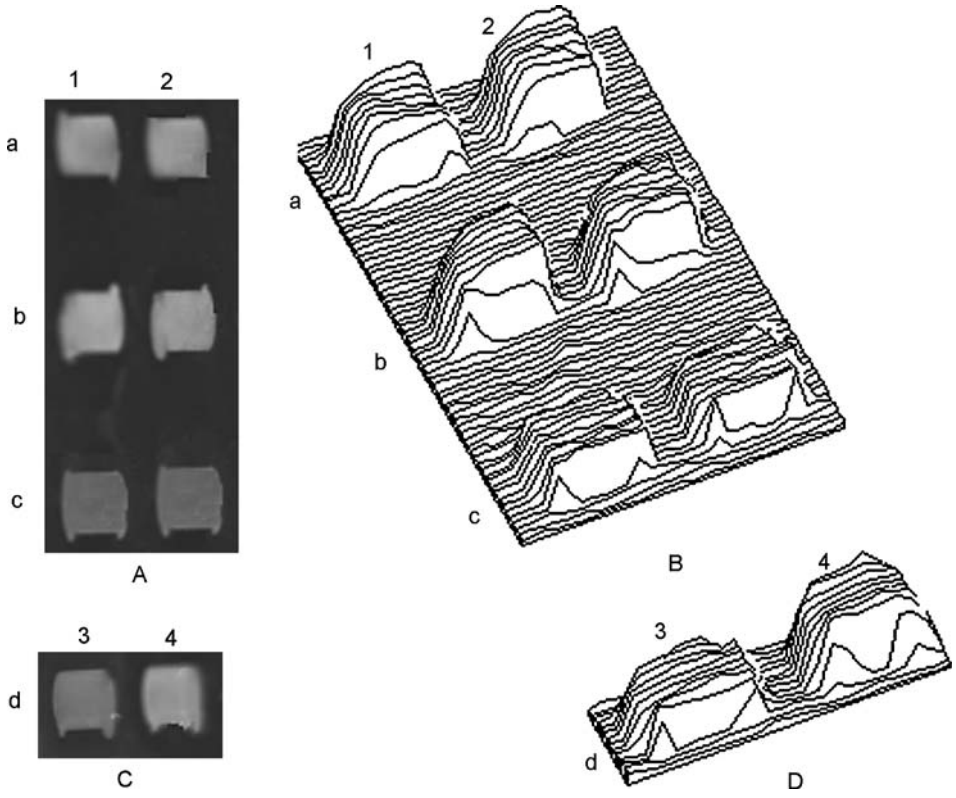


**Fig. 2** Qualitative detection of the antibody and serum sample from SARS patients against SARS-CoV using the biosensor technique based on imaging ellipsometry. (A) The image in grayscale of the microarray biosensor with SARS-CoV and SARS-CoV /antibody complex unit on silicon substrate obtained by imaging ellipsometry; (B) Thickness distribution of the image A in three dimension; (C) An image in grayscale of the microarray biosensor for the detection of serum; (D) Thickness distribution of the image C in three dimension. 1c, 2c and 3d, spots containing SARS-Cov as a control; the surface concentration of the SARS-Cov layer is 0.68 $\mu$g/cm$^2$. 1a and 2a, spots containing antibody h12/SARS-Cov complex layer, the surface concentration of the SARS-Cov layer is 0.9 $\mu$g/cm$^2$. 1b and 2b spots containing antibody b1/SARS-Cov complex layer, the surface concentration of the SARS-Cov layer is 1.14 $\mu$g/cm$^2$. 3d and 4d spots containing serum/SARS-Cov complex layer, the surface concentration of the SARS-Cov layer is 0.96 $\mu$g/cm$^2$

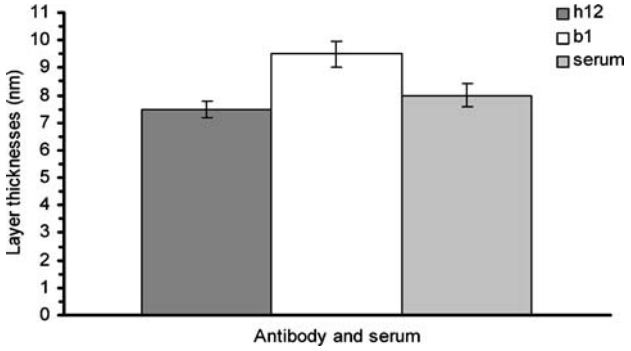


**Fig. 3** Detection of antibody and serum of SARS patient using the biosensor

The result shows that the interaction rate is different for the two binding processes. With the experimental results, we can do a further theoretical analysis. Table 4 shows data detailing the analysis of the kinetic process whereby the antibodies are measured using real-time spectroscopic ellipsometer. The affinity between SARS-CoV and antibody h12 is higher than that with the antibody b1, which demonstrates that different antibodies produce varying levels of affinity between antibodies and virus.

**Table 3** The film thickness of serial serum samples from 10 SARS patients and 12 negative serum samples from volunteers who have not had SARS on biosensor based on imaging ellipsometry

| Negative samples | N1 | N2 | N3 | N4 | N5 | N6 | N7 | N8 | N9 | N10 | N11 | N12 | Mean | SD | Range |
|---|---|---|---|---|---|---|---|---|---|---|---|---|---|---|---|
| Average thickness (nm) | 5.8 | 5.7 | 5.5 | 4.9 | 5.6 | 5.7 | 5.5 | 5.6 | 5.7 | 5.6 | 4.9 | 4.8 | 5.4 | 0.35 | 1 |
| Positive samples | P030 | P026 | P032 | P013 | P010 | P005 | P049 | P004 | P040 | P002 | | | Mean | SD | Range |
| Average thickness (nm) | 11.3 | 12.4 | 13.5 | 9.0 | 11.6 | 7.7 | 5.9 | 10.3 | 11.7 | 6.6 | | | 10 | 2.6 | 7.6 |

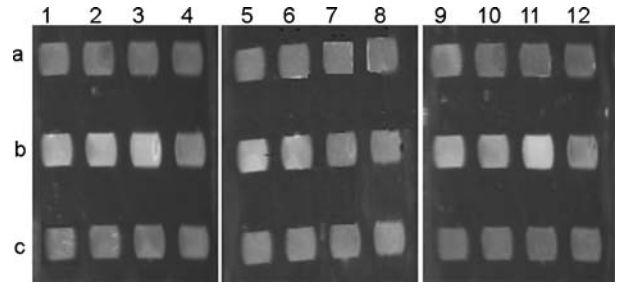


**Fig. 4** Qualitative detection of serum samples from 10 SARS patients and 12 volunteers who have not had SARS using the biosensor based on imaging ellipsometry. a1, a2, a3, a4, a5, a6, a7, a8, a9, a10, a11 and a12 are negative samples N1, N2, N3, N4, N5, N6, N7, N8, N9, N10, N11 and N12; b1, b5, b9 is SARS patient P030; b2, b3, b4, b6, b7, b8, b11 and b22 are SARS patients P026, P032, P013, P010, P005, P049, P004, P040 and P002; c1, c2, c3, c4, c5, c6, c7, c8, c9, c11, c12 spots containing SARS-Cov as a control

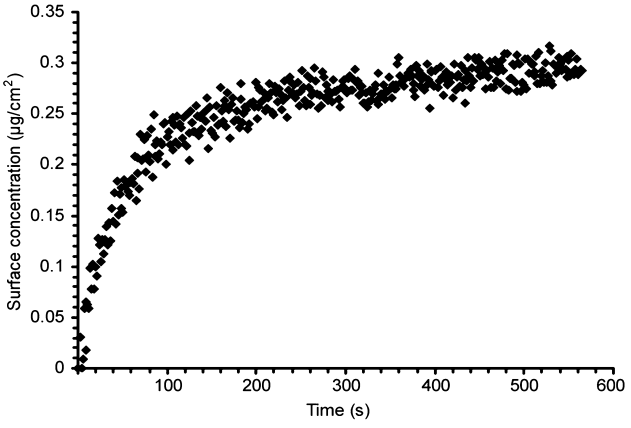


**Fig. 5** The binding process between SARS-CoV and antibody b1 was obtained by real-time spectroscopic ellipsometer. The thickness increased 2.7 nm within 200 s and the corresponding surface concentration increased to 0.324 $\mu$g/cm$^2$. The binding process reached equilibrium within 10 min. $k_a$ is $5.22 \times 10^3$ M$^{-1}$S$^{-1}$, and $k_d$ is 5.5 $\times 10^{-4}$ S$^{-1}$. $K_A$ is $9.5 \times 10^6$ M$^{-1}$

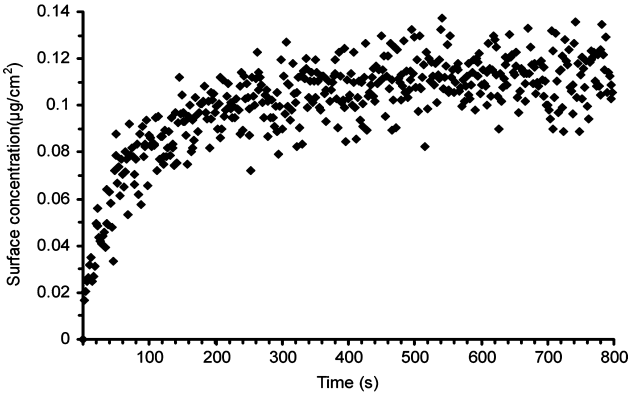


**Fig. 6** The binding process between antibody h12 and SARS-CoV was obtained by real-time spectroscopic ellipsometer. The thickness increased 1.1 nm in 300 s. Surface concentration increased 0.132 $\mu$g/cm$^2$. The binding process reached equilibrium within 10 min. $k_a$ is $7.5 \times 10^3$M$^{-1}$S$^{-1}$, and $k_d$ is $6.6 \times 10^{-4}$S$^{-1}$. $K_A$ is $1.36 \times 10^7$ M$^{-1}$

**Table 4** Data of the kinetic process analysis

| Antibody | $k_a$ | $k_d$ | $K_A$ |
|---|---|---|---|
| Antibody h12 | $7.5 \times 10^3$ M$^{-1}$ S$^{-1}$ | $6.6 \times 10^{-4}$ S$^{-1}$ | $1.36 \times 10^7$ M$^{-1}$ |
| Antibody b1 | $5.22 \times 10^3$ M$^{-1}$ S$^{-1}$ | $5.5 \times 10^{-4}$ S$^{-1}$ | $9.5 \times 10^6$ M$^{-1}$ |

$k_a$ is association rate constant. $k_d$ is dissociation rate constant. $K_A$ is affinity.

## 4. Discussion

Two antibodies might have potential use in the creation of SARS vaccines and in the diagnosis of SARS. We had examined the activity of two scFv fragments selected with phage display. ELISA revealed that the two scFv were specific for SARS-CoV and had a similar level of activity against the SARS-CoV as had the serum from SARS-recovered donors. A significant increase in the attached layer thickness found by the biosensor provided a further indication of the interactive process. The antibodies in the solution interacted on the surface with SARS-CoV and formed into a complex. This point was further reinforced by the kinetic process.

The biosensor based on imaging ellipsometry was valuable diagnostic tools to the accuracy of diagnosis. Compared with other methods, the advantages of the biosensor based on imaging ellipsometry were evident as it didn't require labeling, and provided rapid, visual image detection. The non-use of labels avoided unnecessary disturbance to any bioactivity of analytes. Detection of neutralizing antibody in 10 serum samples from SARS-infected donors using the biosensor showed different concentration also. ELISA required labeling of the samples, which might affect the activity of the antibodies. The presence of the second antibody and the dye directly might affect OD. ELISA occasionally produced false positives (Wang et al., 2004a). The biosensor and real-time analysis could detect directly the thickness of the antibodies' layer with no labeling. The biosensor demonstrated the fact that antibodies b1 and h12 had different level of activity in encountering the virus. In addition, the biosensor can performed multiple tests simultaneously, thus the biosensor with a microarray was much more convenient to analyze the two antibodies.

The real-time analysis was a utility and intuitionistic experimental tool. The affinity of the two antibodies encountering the SARS-CoV was deduced using real-time measurement. Different antibodies exhibited different levels of capacity to neutralize the SARS-CoV. The function of real-time analysis was to supply some important kinetic data, such as the interaction rate, affinity, conditions, etc. This kinetic data provided important information for the understanding of the antigenicity and immunogenicity of the SARS-CoV. Clearly defining interaction characteristics ensured that the best antibodies were selected as research tools or assay components. Two antibodies against the SARS-CoV proved to be

an effective antidote to the virus and they might have practical application beyond simple clinical diagnosis. These antibodies might be also used to help unravel the details of biological mechanisms of the SARS-CoV and identify therapeutic targets.

As a label-free immunological method, the biosensor has been applied in the antibodies b1 and h12 interaction with SARS-CoV. It proves that the antibody b1 and h12 have the capacity to neutralize SARS-CoV. The kinetic data of antibody against SARS-CoV can also elucidate disease mechanisms and the antigenicity and immunogenicity of the SARS-CoV. Therefore, the biosensor is a valuable diagnostic tool with a high accuracy and available to a clinician in concert with conventional test methods.

## Acknowledgments

The Chinese Academy of Sciences and National Natural Science Foundation of China (NSFC) are gratefully acknowledged for their supports.

## References

H. Arwin, S. Welin-Klintström, and R. Jansson, J. Colloid Interface Sci **156**, 337 (1993).
H. Bisht, A. Roberts, L. Vogel, A. Bukreyev, P.L. Collins, B.R. Murphy, et al., Proc. Natl. Acad Sci USA **101**, 6641 (2004).
A. Bukreyev, E.W. Lamirande, U.J. Buchholz, L.N. Vogel, W.R. Elkins, M.S.T. Claire, et al., Lancet **363**, 2122 (2004).
J.Z. Duan, X.Y. Yan, X. M. Guo, W.C. Cao, W. Han, Cai Qi, et al., Biochemical and Biophysical Research Communications **333**, 186 (2005).
J.Z. Duan, X. Ji, J. Feng, W. Han, P.H. Zhang, W.C. Cao, et al., Antiviral Therapy **11**, In press (2006).
O. Hofmann, G. Voirin, P. Niedermann, and A. Manz, Anal Chem **74**, 5243 (2002).
G. Jin, R. Jansson, I. Lundstrom, and H. Arwin, Transducer'95 Eurosensors IX (1995a).
G. Jin, R. Jansson, and H. Arwin, Rev Sci Instrum **67**, 2930 (1996).
G. Jin, P. Tengvall, I. Lundstrom, and H. Arwin, Anal Biochem **232**, 69 (1995b).
G. Jin, Z.H. Wang, C. Qi, Z.Y. Zhao, S. Chen, Y.H. Meng, et al., Proceedings of the 25th annual international conference of the IEEE EMBS, Cancun Mexico, 3575 (2003).
J.R. Lingappa, L.C. McDonald, P. Simone, and U.D. Parashar, http://www.cdc. gov/ncidod/EID/v- ol10no2/03-1032.htm (2004).
L.T. Lau, Y.W.W. Fung, F.P.F. Wong, S.S. Lin, C.R. Wang, H.L. Li, et al., Res. Commun **312**, 1290 (2003).
W.H. Long, H.S. Xiao, X.M. Gu, Q.H. Zhang, H.J. Yang, G.P. Zhao, et al., J Virol Methods **121**, 57 (2004).
Y. Lin, X. Yan, W. Cao, C. Wang, J. Feng, J. Duan, et al., Antivir Ther **9**, 287 (2004).
A.C. Malmborg, A. Michaelsson, M. Ohlin, B. Janaaon, and C.K. Borremaeck, Scand. J Immunol **35**, 643 (1992).
Y. Oba, Engl J Med **348**, 2034 (2003).
J.S.M. Peiris, S.T. Lai, L.L.M. Poon, Y. Guan, L.Y. Yam, W. Lim, et al., Lancet **361**, 1319 (2003).
S.M. Poutanen, D.E. Low, B. Henry, S. Finkelstein, D. Rose, K. Green, R. Tellier, et al., New Engl J Med **348**, 1995 (2003).
L.L. Poon, B.W. Wong, K.H. Chan, C.S. Leung, K.Y. Yuen, Y. Guan, et al., J Clin Virol **30**, 214 (2004).
M. Stenberg and H. Nygren, Journal de Physique **44**, 83 (1983).
J. Ter Meulen, A.B. Bakker, E.N. Van den Brink, G.J. Weverling, B.E. Martina, B.L. Haagmans, et al., Lancet **363**, 2139 (2004).
H. Wang, Y. Ding, X. Li, L. Yang, W. Zhang, and W. Kang, N Engl J Med **349**, 507 (2003a).
Y.D. Wang, Y. Li, G.B. Xu, X.Y. Dong, X.A. Yang, Z.R. Feng, et al., Clin. Immunol **113**, 145 (2004a).
Z.H. Wang and G. Jin, J Immunol Methods **285**, 237 (2004b).
Z.H. Wang and G. Jin, Chinese Journal of Biotechnology **18**, 99 (2002).
Z.H. Wang and G. Jin, Anal Chem **75**, 6119 (2003b).
Z.H. Wang and G. Jin, J Biochem Biophys Methods **57**, 203 (2003c).
Z.H. Wang and G. Jin, Colloids Surf. B: Biointerf **34**, 173 (2004c).
Q. Wu, Z. Xu, T. Wei, H. Zeng, J. Li, H. Gang, et al., J Virol Methods **119**, 17 (2004).
Z.Y. Yang, W.P. Kong, Y. Huang, A. Roberts, B.R. Murphy, K. Subbarao, et al., Nature **428**, 561 (2004).
Y.Y. Yu, B.J. Van Wie, A.R. Koch, D.F. Moffett, and W.C. Davis, Anal Biochem **263**, 158 (1998).
P.Q. Ying, G. Jin, and Z.L. Tao, 2nd European Medical and Biological Engineering Conference, Vienna, 190 (2002).
P.Q. Ying, G. Jin, and Z.L. Tao, Colloids Surf. B: Biointerf **33**, 259 (2004).
Z.Y. Zhao, G. Jin, and Z.H. Wang, 20th International conference of the IEEE Engineering in Medicine and Biology Society, Hong Kong, 269 (1998).
H.G. Zhang, C. Qi, Z.H. Wang, G. Jin, and R.J. Xiu, Clin Chem **51**, 1038 (2005).